

## Pyrazolylborate–Zinc–Nucleobase-Complexes, 3:1 Base Pairing Studies

Dirk Badura and Heinrich Vahrenkamp\*

Institut für Anorganische und Analytische Chemie der Universität Freiburg, Albertstr. 21,  
D-79104 Freiburg, Germany

Received April 17, 2002

In solution, the pyrazolylborate–zinc–nucleobase complexes show self-association and base pairing with external nucleobases. The self-association was studied quantitatively for  $\text{Tp}^{\text{Cum,Me}}\text{Zn}$ –hypoxanthinate and  $\text{Tp}^{\text{Cum,Me}}\text{Zn}$ –thymine; the dimerization constants  $K_D$  are  $63 \pm 8$  and  $0.2 \pm 0.1 \text{ M}^{-1}$ , respectively. Of the external nucleobases, 9-ethyladenine forms stable base pairs with the thymine, uracil, and xanthinate complexes, 9-isobutylguanine only with the cytosine complex, 1-methylthymine with the adenine and diaminopurinate complexes, and 1-methyluracil with the diaminopurinate complex. The association constant for the base pair  $\text{Tp}^{\text{Cum,Me}}\text{Zn}$ –thymine:9-ethyladenine was determined by NMR methods as  $K = 66 \pm 10 \text{ M}^{-1}$ . Structure determinations of the crystalline adducts have confirmed the base pairing for  $\text{Tp}^{\text{Cum,Me}}\text{Zn}$ –thymine:9-ethyladenine,  $\text{Tp}^{\text{Cum,Me}}\text{Zn}$ –cytosine:9-isobutylguanine, and  $\text{Tp}^{\text{Cum,Me}}\text{Zn}$ –xanthinate:9-ethyladenine. Both Watson–Crick and Hoogsteen base pairs have been observed. In the solid state, extended base pairing leads to quartet and polymer arrangements.

### Introduction

Base pairing between nucleotides, which is the essence of all genetic processes, is affected in many ways by the presence of metal ions.<sup>2,3</sup> In a positive sense, they are essential for the stability of the DNA helices; in a negative sense, their coordination to the nucleobases can cause mutations. The best known application of this is the medical use of cisplatin,<sup>4</sup> that is, the blocking of replication, transcription, or translation through metal coordination. In our research field, zinc chemistry, one of the earliest observations of this kind was made in 1968 by Eichhorn: zinc ions were found to impede the melting of DNA by stabilizing the double helix through metal coordination at the phosphate residues. Conversely, upon cooling, zinc ions facilitate the complete recombination of the double helix by favorable coordination at the nucleobases.<sup>5,6</sup>

While the relevance of this topic, metals in genetics, has generated many papers on the interactions of metal ions with nucleotides, nucleic acids, and their constituents,<sup>2–4</sup> the amount of zinc chemistry in this field is still rather limited.<sup>7</sup> More specifically, the base pairing properties of zinc-bound nucleobases seem to be virtually unknown, with two older studies<sup>8,9</sup> lacking the necessary sophistication.

Motivated by this, we have undertaken an extensive study of zinc–nucleobase interactions. To limit the acceptor properties of zinc to one coordination site and to ensure stability and inertness of the complexes, we applied zinc complexes with encapsulating pyrazolylborate ligands  $\text{Tp}^*$ , specifically  $\text{Tp}^{\text{Cum,Me}}\text{Zn}$  and  $\text{Tp}^{\text{Ph,Me}}\text{Zn}$  units. In the preceding paper,<sup>1</sup> we have outlined our objectives, listed the leading references, and described the syntheses and structures of  $\text{Tp}^*\text{Zn}$  complexes with nine nucleobases. The nucleobases are always attached to zinc in their anionic forms via nitrogen atoms. In seven of the nine cases, the zinc ion is bound at the nitrogen which in the nucleosides bears the sugar moiety, thus making the  $\text{Tp}^*\text{Zn}$ –nucleobase complexes analogues of the nucleosides.

The latter property makes it likely that the complexes are amenable to base pairing. In accord with this, all structure

\* To whom correspondence should be addressed. E-mail: vahrenka@uni-freiburg.de.

- (1) Part 2, preceding paper: Badura, D.; Vahrenkamp, H. *Inorg. Chem.* 2001, 40, 6013.
- (2) Saenger, W. *Principles of Nucleic Acid Structure*; Springer: New York, 1984.
- (3) *Interactions of Metal Ions with Nucleotides, Nucleic Acids and their Constituents*; Sigel, H., Ed.; Metal Ions in Biological Systems, Vol. 32; Marcel Dekker: New York, 1996.
- (4) Lippert, B. *Prog. Inorg. Chem.* 1989, 37, 1.
- (5) Shin, Y. A.; Eichhorn, G. L. *Biochemistry* 1968, 7, 1026.
- (6) Eichhorn, G. L.; Shin, Y. A. *J. Am. Chem. Soc.* 1968, 90, 7323.

(7) For the leading references, see ref 1.

(8) Wang, S. M.; Li, N. C. *J. Am. Chem. Soc.* 1968, 90, 5069.

(9) Ghose, R. *Inorg. Chim. Acta* 1989, 156, 303.

determinations revealed that in the solid state the complexes are hydrogen-bonded dimers.<sup>1,10</sup> The preliminary observation that free nucleobases can become soluble in nonpolar media in the presence of zinc–nucleobase complexes<sup>10</sup> also pointed in this direction. We therefore studied the interactions between the  $\text{Tp}^*\text{Zn}$ –base complexes themselves and with additional nucleobases and nucleoside analogues, hoping to identify the base pairing patterns and to obtain qualitative and quantitative data on the strength of the base pairing.

## Results and Discussion

Of the eight types of  $\text{Tp}^*\text{Zn}$ –nucleobase complexes described in the preceding paper, seven were found to be suitable for base pairing studies: those with thymine, uracil, cytosine, adenine, diaminopurine, xanthine, and hypoxanthine. Being analogues of the nucleosides, they should, in principle, be able to form all kinds of base pairs which have been observed for the nucleosides themselves. This should start with self-association, should include the Watson–Crick combinations as prominent examples, and should extend to the nonnatural base pairing schemes.

As shown in the preceding paper, self-association is a common feature of all the complexes. The investigations for the present paper showed, however, that base pairing between the  $\text{Tp}^*\text{Zn}$ –nucleobase complexes and external free nucleobases is not strong enough to overcome the competing base pairing, that is, that between the free nucleobases themselves. With a few exceptions, the free nucleobases did not dissolve in solutions of the  $\text{Tp}^*\text{Zn}$ –nucleobase complexes in nonprotic media, and we could not isolate or identify in solution a  $\text{Tp}^*\text{Zn}$ –nucleobase:nucleobase adduct. We therefore resorted to using *N*-alkylated nucleobases, which just like the  $\text{Tp}^*\text{Zn}$ –nucleobase complexes are analogues of the nucleosides. Thus, all base pairs described in this paper are analogues of base pairing combinations between nucleosides.

**Self-Association.** In the previous work,<sup>1,10</sup> we had determined the solid state structures of seven types of  $\text{Tp}^*\text{Zn}$ –nucleobase complexes. Six of these are dimers, held together by a pair of hydrogen bonds between the nucleobases across an inversion center. According to this, monomer–dimer equilibria should exist for the complexes in solution. With one exception, however, the standard  $^1\text{H}$  NMR spectra showed no evidence for this: either all C–H proton resonances of the monomers and the dimers have the same chemical shifts or a rapid exchange averages them out. This picture did not change upon diluting or cooling the solutions.

The exceptions are the two hypoxanthine complexes  $\text{Tp}^{\text{Cum,Me}}\text{Zn}$ –HYX' and  $\text{Tp}^{\text{Ph,Me}}\text{Zn}$ –HYX'.<sup>1</sup> Figure 1 shows the variable temperature NMR spectra of  $\text{Tp}^{\text{Cum,Me}}\text{Zn}$ –HYX' in the 6–8 ppm range where the changes are most noticeable. The resonances marked as 1 correspond to the pyrazole C–H, those marked as 2, to C<sup>8</sup>–H of hypoxanthine. As such, the data do not prove a monomer–dimer equilibrium, because an isomerization equilibrium might also exist, for example, between N<sup>7</sup>- and N<sup>9</sup>-bound hypoxanthine. This latter possibility was excluded by a dilution series. As

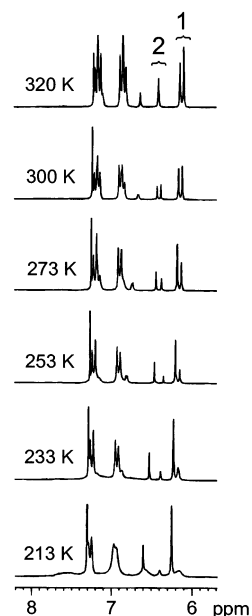


**Figure 1.** Variable temperature  $^1\text{H}$  NMR spectra of  $\text{Tp}^{\text{Cum,Me}}\text{Zn}$ –HYX' in the 6–8 ppm range.

expected for a monomer–dimer equilibrium, upon dilution at a given temperature, the relative concentration of the monomer grows. This way, the monomer and the dimer were identified consistently with the observation that the dimer prevails at low temperatures. The NMR spectra show that near room temperature the number of protons in the monomer and the dimer is the same. From this and the total concentration in the NMR solution, according to the formulations given in the following equations, the dimerization constant  $K_D$  can be calculated as  $63 \pm 8 \text{ M}^{-1}$ .

The N–H proton resonances of  $\text{Tp}^{\text{Cum,Me}}\text{Zn}$ –HYX' in the 9–14 ppm range, which broaden very much at lower temperatures, confirm the existence of a monomer–dimer equilibrium. The signal for the monomer at 8.7 ppm moves slightly downfield upon cooling and disappears at 240 K. The signal for the dimer, typically further downfield than that of the monomer, moves from 10.4 to 13.2 ppm upon cooling to 213 K.

In all other cases, the N–H proton resonances of the nucleobases were the only indicators of monomer–dimer equilibria. Quantitative data on self-association were obtained from them for the thymine complex  $\text{Tp}^{\text{Cum,Me}}\text{Zn}$ –T'. This was done by recording the chemical shift  $\delta_{\text{obs}}$  for the N<sup>3</sup>–H proton of thymine for a dilution series. In this case, there is only one NMR signal, representing an average chemical shift for the monomer and the dimer. This chemical shift,  $\delta_{\text{obs}}$ , can be related to the two individual chemical shifts,  $\delta_0$  for the monomer and  $\delta_{\text{BP}}$  for the base pair (i.e., the dimer), according to eq 3 in which the factor  $f$  is the ratio of the dimer concentration  $[\text{D}]$  and the total concentration  $[\text{A}_T]$ . Equations 1–4 display the definitions. Taking into account the mass balance, eqs 5, 2, and 4 yield eq 6.<sup>11</sup> Finally, the combination of eqs 3 and 6 yields eq 7, giving the relation

(10) Ruf, M.; Weis, K.; Vahrenkamp, H. *Inorg. Chem.* **1997**, *36*, 2130.

(11) Connors, K. A. *Binding Constants*; Wiley: New York, 1987.

between the only observable ( $\delta_{\text{obs}}$ ) and the only known quantity ( $[A_T]$ ).



$$K_D = \frac{[D]}{[A]^2} \quad (2)$$

$$\delta_{\text{obs}} = \delta_0 + f(\delta_D - \delta_0) \quad (3)$$

$$f = \frac{[D]}{[A_T]} \quad (4)$$

$$[A_T] = [D] + 2[A] \quad (5)$$

$$f = \frac{[D]}{[A_T]} = \frac{1 + 4K_D A_T - \sqrt{1 + 8K_D A_T}}{4K_D A_T} \quad (6)$$

$$\delta_{\text{obs}} = \delta_0 + (\delta_{\text{BP}} - \delta_0) \frac{1 + 4K_D A_T - \sqrt{1 + 8K_D A_T}}{4K_D A_T} \quad (7)$$

Figure 2 displays the relation between these two quantities as obtained from the NMR measurements. Least-squares analysis of the data<sup>12</sup> produced the values  $\delta_0 = 6.89 \pm 0.05$  ppm,  $\delta_{\text{BP}} = 10.75 \pm 0.5$  ppm, and  $K_D = 0.2 \pm 0.1 \text{ M}^{-1}$  with a correlation coefficient of 0.988. Of these,  $\delta_0$  is close to being an experimental value, cf. Figure 2, while  $\delta_{\text{BP}}$  is far beyond the measuring range. This fact also means that saturation was not reached in the measuring range which would have proved that the application of eq 7 is appropriate. However, the good fit of the data for 2 orders of magnitude in  $[A_T]$  lends support to the correctness of the applied model, the large error margin of  $K_D$  expresses the uncertainties in its determination, and the resulting value of the dimerization constant is intuitively correct: it is much smaller than that of  $\text{Tp}^{\text{Cum,MeZn}}-\text{HYX}'$ , and it is also an order of magnitude smaller than that of 1-methylthymine,<sup>13</sup> the simplest analogous nucleoside derivative, thereby indicating the significant influence of the voluminous pyrazolylborate moiety.

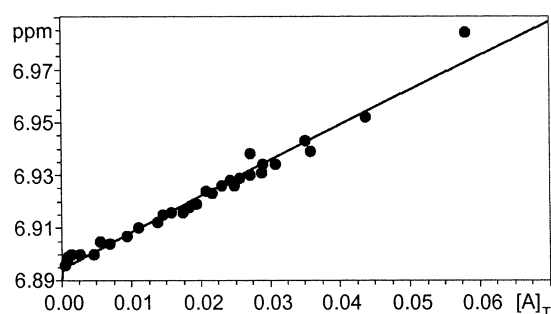


**Figure 2.** Plot of  $\delta_{\text{obs}}$  for the thymine  $\text{N}^3\text{-H}$  (in  $\text{CDCl}_3$ ) against the total concentration for  $\text{Tp}^{\text{Cum,MeZn}}-\text{T}'$ .

The chemical shift effects for the  $\text{N-H}$  protons of the other  $\text{Tp}^*\text{Zn}$ -nucleobase complexes which are involved in self-associative base pairing are similar to those of  $\text{Tp}^{\text{Cum,MeZn}}-$

$\text{T}'$ , thereby confirming a certain, yet small, degree of self-association in solution. This raised hopes that Watson-Crick-like base pairing should be identifiable for pairs of complementary  $\text{Tp}^*\text{Zn}$ -nucleobase complexes, that is,  $\text{Tp}^*\text{Zn}-\text{A}' + \text{Tp}^*\text{Zn}-\text{T}'$  or  $\text{Tp}^*\text{Zn}-\text{DAP}' + \text{Tp}^*\text{Zn}-\text{X}'$ . We failed, however, to collect convincing evidence for this. The  $^1\text{H}$  NMR spectra of mixtures of pairs of  $\text{Tp}^*\text{Zn}$ -nucleobase complexes, most typically  $\text{Tp}^{\text{Ph,MeZn}}-\text{A}' + \text{Tp}^{\text{Ph,MeZn}}-\text{T}'$ , just show the two individual components. There are shifts of the hydrogen bonding  $\text{N-H}$  protons upon dilution, but again not significantly different from those of the individual complexes. Finally, crystallization of 1:1 mixtures of complementary complexes did not yield crystals containing both components.

**Pairing with Nucleobases.** Proton NMR spectroscopy of the  $\text{NH}$  functions involved in hydrogen bonding was also the method of choice for the detection of base pairing between the  $\text{Tp}^*\text{Zn}$ -nucleobase complexes and additional nucleobases. The bases employed, which are all analogues of the corresponding nucleosides, were 9-isobutylguanine (Bu-G), 1-isopropylcytosine (Pr-C), 9-ethyladenine (Et-A), 1-methylthymine (Me-T), 1-methyluracil (Me-U), and 1-isopropylthymine (Pr-T). They were combined with those  $\text{Tp}^*\text{Zn}$ -nucleobase complexes with which Watson-Crick or Hoogsteen base pairing might be expected. The large number of possible combinations was limited further by the fact that not all NMR signals of the relevant  $\text{NH}$  protons are observable in the chosen solvent,  $\text{CDCl}_3$ . Altogether, the combinations listed in Table 1 were investigated.

**Table 1.**  $^1\text{H}$  NMR Association Shifts for Those  $\text{N-H}$  Protons of the  $\text{Tp}^*\text{Zn}$ -Nucleobase Complexes Which Are Involved in Hydrogen Bonding between  $\text{Tp}^*\text{Zn}$ -Nucleobase Complexes and Free Nucleobases

complex	conc, mM	NH or $\text{NH}_2$	base	ratio base/complex	$\Delta$ , ppm
$\text{Tp}^{\text{Cum,MeZn}}-\text{T}'$	0.017	$\text{N}^3\text{H}$	Bu-G	1.0	
	0.009	$\text{N}^3\text{H}$	Pr-C	1.2	0.01
	0.025	$\text{N}^3\text{H}$	Et-A	1.0	1.76
$\text{Tp}^{\text{Ph,MeZn}}-\text{T}'$	0.025	$\text{N}^3\text{H}$	Et-A	1.0	1.27
$\text{Tp}^{\text{Cum,MeZn}}-\text{U}'$	0.031	$\text{N}^3\text{H}$	Bu-G	1.0	
	0.025	$\text{N}^3\text{H}$	Et-A	1.0	1.36
$\text{Tp}^{\text{Cum,MeZn}}-\text{C}'$	0.003	$\text{NH}_2$	Bu-G	1.0	1.19
$\text{Tp}^{\text{Cum,MeZn}}-\text{A}'$	0.017	$\text{NH}_2$	Bu-G	1.0	
	0.009	$\text{NH}_2$	Pr-C	1.6	0.03
	0.025	$\text{NH}_2$	Me-T	1.0	0.23
$\text{Tp}^{\text{Ph,MeZn}}-\text{A}'$	0.025	$\text{NH}_2$	Me-T	1.0	0.22
	0.023	$\text{NH}_2$	Me-U	1.0	0.20
$\text{Tp}^{\text{Ph,MeZn}}-\text{DAP}'$	0.023	$\text{N}^2\text{H}_2$	Me-T	1.1	0.68
		$\text{N}^6\text{H}_2$			0.79
$\text{Tp}^{\text{Cum,MeZn}}-\text{X}'$	0.034	$\text{N}^1\text{H}$	Bu-G	1.0	
	0.006	$\text{N}^1\text{H}$	Pr-C	1.3	0.01
	0.009	$\text{N}^1\text{H}$	Pr-T	1.0	0.04
		$\text{N}^3\text{H}$			0.24
	0.012	$\text{N}^1\text{H}$	Et-A	1.0	0.07
	$\text{N}^3\text{H}$			0.88	

As mentioned previously and as observed here again, the proton signals of all CH units of the involved species do not shift upon base pairing interactions. Yet, the signals of the  $\text{NH}$  protons involved in hydrogen bonding can show shifts of up to several ppm. In a first approximation, these relative shifts, when taken for the same  $\text{NH}$  containing compound under the same conditions, can be taken as a measure of the amount of base pairing, that is, the position of the base pairing equilibrium, irrespective of the other base

(12) Hyams, D. *CURVE EXPERT*, version 1.34; Starkville, MS 39759, 1995–1997.

(13) Kyogoku, Y.; Lord, R. C.; Rich, A. *Proc. Natl. Acad. Sci. U.S.A.* **1967**, *57*, 250; *J. Am. Chem. Soc.* **1967**, *89*, 496.

used for pairing.<sup>14</sup> We worked this way by using  $\text{CDCl}_3$  as the solvent (except for the  $\text{Tp}^{\text{Cum,Me}}\text{Zn}-\text{C}'/9\text{-isobutylguanine}$  combination in  $\text{CD}_3\text{CN}$ ), by keeping the  $\text{Tp}^*\text{Zn}$ –nucleobase concentration in the 0.01–0.03 M range, and by recording the shifts of those NH resonances of the  $\text{Tp}^*\text{Zn}$ –nucleobase complexes which are involved in the base pairing for zinc complex/base molar ratios near 1. Table 1 lists the relevant data. The significant information is in the last column giving the  $\Delta$  value, that is, the shift of the hydrogen bonding proton signal(s) relative to the signal(s) for the zinc complex alone.

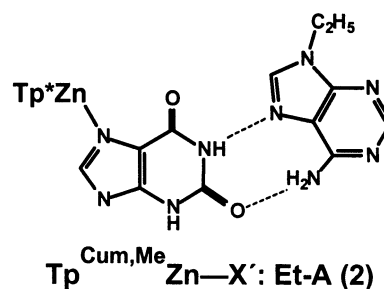
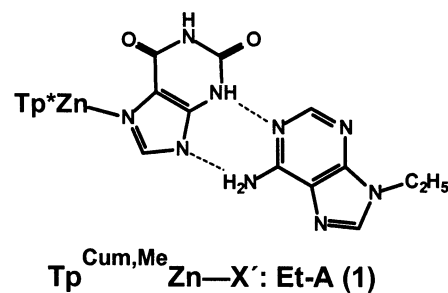
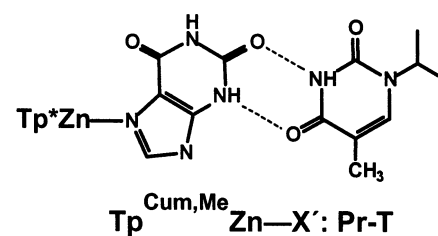
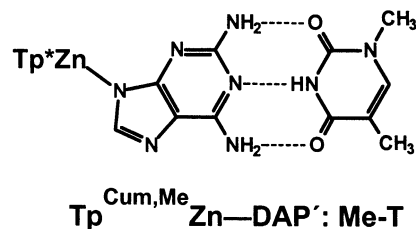
Table 1 shows that there is a high preference for the “natural” base pairing combinations, that is, A:T or A:U and G:C. The first entries in the table, that is, those for  $\text{Tp}^*\text{Zn}-\text{T}'$ , can be taken as representative examples. 9-Isobutylguanine does not combine with any other complex than the cytosine complex, even at higher concentrations. Because of the nonexistence of a  $\text{Tp}^*\text{Zn}$ –guanine complex, 1-isopropylcytosine does not find a good partner and becomes only very weakly coordinated. 9-Ethyladenine, however, is a very good partner for the thymine and uracil complexes. In turn, 1-methylthymine and 1-methyluracil are the correct partners for the adenine complexes. The  $\text{Tp}^*\text{Zn}-\text{DAP}'\text{:Me-T}$  or Me-U combination is a nonnatural, yet favorable, one as it allows a triple hydrogen bonding interaction. Finally, the lanthinate complex goes along reasonably well with 1-isopropylthymine and very well with 9-ethyladenine.

Structural information on the resulting base pairs could be extracted from the NMR data in only a few cases by also analyzing the NH signal shifts of the added nucleobases. In the various A:T and A:U combinations, the relevant signal of the added base ( $\text{NH}_2$  for 9-ethyladenine and  $\text{N}^3\text{H}$  for 1-methylthymine or 1-methyluracil) also undergoes a shift of up to 0.4 ppm. This is, however, not enough information to distinguish between Watson–Crick or Hoogsteen base pairing. Information on the C:G combination is not available because the NH proton resonances of 9-isobutylguanine are not observable in the mixture. For the  $\text{Tp}^{\text{Ph,Me}}\text{Zn}-\text{DAP}'\text{:Me-T}$  combination, the NMR data correspond to expectation. Both  $\text{NH}_2$  groups of the diaminopurine are involved in equally strong hydrogen bonding interactions, see Table 1. At the same time,  $\text{N}^3\text{H}$  of 1-methylthymine experiences a coordination shift of about 2 ppm. Thus, the triply bridged aggregates as shown below should be the prevailing species in solution. The only case where one out of two alternatives is clearly preferred is the  $\text{Tp}^{\text{Cum,Me}}\text{Zn}-\text{X}'\text{:Pr-T}$  combination. As Table 1 shows, the xanthinate ligand uses  $\text{N}^3\text{H}$  for hydrogen bonding. At the same time, the  $\text{N}^3\text{H}$  signal of 1-isopropylthymine shifts by 0.2 ppm. This way, the two NH groups involved in hydrogen bonding are identified. Yet, this still leaves four possible modes of association, depending on whether  $\text{O}^2$  or  $\text{N}^9$  of xanthine and  $\text{O}^2$  or  $\text{O}^4$  of 1-isopropylthymine are the hydrogen bond acceptors. One of them is shown here, being chosen because of the preference of thymine to use  $\text{O}^4$  for hydrogen bonding<sup>15</sup> and the observation of the small shift of the xanthine  $\text{N}^1\text{H}$  upon association.

(14) Katz, L. *J. Mol. Biol.* **1969**, *44*, 279.

(15) *Basic Principles of Nucleic Acid Chemistry*; Ts'o, P. O. P., Ed.; Academic Press: New York, 1974; Vol. 1, pp 453–584.

Finally, the NMR data for the  $\text{Tp}^{\text{Cum,Me}}\text{Zn}-\text{X}'\text{:Et-A}$  combination are puzzling. They indicate that both  $\text{N}^1\text{H}$  and  $\text{N}^3\text{H}$  of the xanthinate are involved in hydrogen bonding. This cannot be in a base pair with adenine and, hence, seems to indicate that two different types of hydrogen bonded association are present in solution at the same time which are denoted by (1) and (2) in the formula drawings.



Quantitative information on the extent of association was obtained for the  $\text{Tp}^{\text{Cum,Me}}\text{Zn}-\text{T}'\text{:Et-A}$  base pair. The coordination shift  $\Delta$  in Table 1 indicated that there is a strong interaction. As determined here for  $\text{Tp}^{\text{Cum,Me}}\text{Zn}-\text{T}'$  and previously for 9-ethyladenine,<sup>16</sup> the self-association constants for the two components of the base pair (0.2 and  $1.4 \text{ M}^{-1}$ , respectively) are comparatively small. Hence, their self-association should not seriously affect the NMR shifts resulting from the base pairing. The measuring procedure

(16) Nagel, G. M.; Hanlon, S. *Biochemistry* **1972**, *11*, 816.



corresponded to that used for  $\text{Tp}^{\text{Cum,Me}}\text{Zn}-\text{T}'$ . Small portions of a 0.1 M solution of 9-ethyladenine (abbreviated as B') were added to a 0.01 M solution of  $\text{Tp}^{\text{Cum,Me}}\text{Zn}-\text{T}'$  (abbreviated as TpB), and a  $^1\text{H}$  NMR spectrum was recorded for each interval, measuring the chemical shift of the  $\text{N}^3\text{H}$  signal of TpB. The system under investigation is defined by eqs 8–11, again with  $\delta_0$  as the known chemical shift for pure TpB and  $\delta_{\text{BP}}$  the unknown chemical shift of the base pair.



$$K_{11} = \frac{[\text{BP}]}{[\text{TpB}][\text{B}']} \quad (9)$$

$$\delta_{\text{obs}} = \delta_0 + f(\delta_{\text{BP}} - \delta_0) \quad (10)$$

$$f = \frac{[\text{BP}]}{[\text{TpB}]_{\text{T}}} \quad (11)$$

$$\Delta = \delta_{\text{obs}} - \delta_0 \quad (12)$$

$$\Delta_{11} = \delta_{\text{obs}} - \delta_0 \quad (13)$$

$$\Delta = f \cdot \Delta_{11} = \frac{\Delta_{11}K_{11}[\text{B}']}{1 + K_{11}[\text{B}']} \quad (14)$$

$$[\text{B}'] = [\text{B}']_{\text{T}} - [\text{BP}] \quad (15)$$

$$[\text{BP}] = [\text{TpB}]_{\text{T}} \frac{\Delta}{\Delta_{11}} \quad (16)$$

$$\frac{[\text{B}']_{\text{T}}}{\Delta} = \frac{[\text{B}']_{\text{T}} + [\text{TpB}]_{\text{T}} - [\text{BP}]}{\Delta_{11}} + \frac{1}{\Delta_{11}K_{11}} \quad (17)$$

The analysis of the data followed the procedure outlined by Nakano,<sup>17</sup> which requires that about 80% of the maximum chemical shift is observed. This requires a large excess of the base component, in our case at least 20-fold, which could be realized. The necessary transformations of the equations<sup>11</sup> are given as eqs 12 and 13, defining relative chemical shifts  $\Delta$ . Substitution of 11–13 into 9 generates 14, relating the measured quantity  $\Delta$  to the desired quantity  $K_{11}$ . Taking the mass balance (eq 15) into account and substituting  $[\text{BP}]$  according to 16 generates eq 17 which is the y-reciprocal form of 14. Equation 17 contains the three unknown quantities  $K_{11}$ ,  $[\text{BP}]$ , and  $\Delta_{11}$ . To get a first approximation of their values,  $[\text{B}']/\Delta$  is plotted against  $([\text{B}']_{\text{T}} + [\text{TpB}]_{\text{T}})$ . The slope of the corresponding least-squares line gives a starting value for  $1/\Delta_{11}$ . This can be used to calculate a starting value of  $[\text{BP}]$  from eq 16. Now, a first plot of  $[\text{B}']/\Delta$  against  $([\text{B}']_{\text{T}} + [\text{TpB}]_{\text{T}} - [\text{BP}])$  can be made, yielding a better value of  $1/\Delta_{11}$ . Fivefold iteration of this procedure yielded a constant value of  $1/\Delta_{11}$ , corresponding to  $1/\Delta_{11} = 0.219$  and  $\Delta_{11} = 4.57$  ppm. Figure 3 shows the final plot. Its intercept corresponds to  $1/(\Delta_{11}K_{11}) = 0.0033$  with a

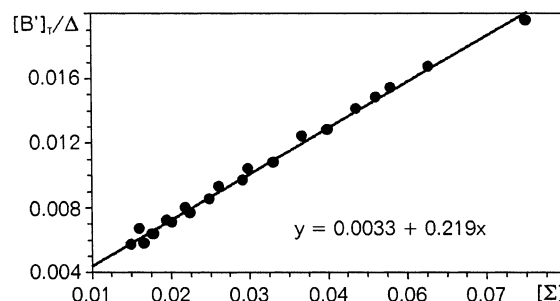


**Figure 3.** Plot according to eq 17 for the titration of  $\text{Tp}^{\text{Cum,Me}}\text{Zn}-\text{T}'$  with 9-ethyladenine.  $\Sigma = [\text{B}']_{\text{T}} + [\text{TpB}]_{\text{T}} - [\text{BP}]$ .

correlation coefficient of 0.998. This transforms into the desired equilibrium constant  $K_{11} = 66 \pm 10 \text{ M}^{-1}$ .

The association constant of  $66 \text{ M}^{-1}$  compares reasonably well with those for the base pairs 1-cyclohexylthymine:9-ethyladenine ( $130 \pm 36 \text{ M}^{-1}$ )<sup>13</sup> and 1-cyclohexyluracil:9-ethyladenine ( $74 \pm 6 \text{ M}^{-1}$ ).<sup>16</sup> Thus, in this case, there is no significant steric hindrance by the  $\text{Tp}^*$  substituents, and the association is much stronger than that between two  $\text{Tp}^*\text{Zn}$ -nucleobase complexes (except  $\text{Tp}^{\text{Cum,Me}}\text{Zn}-\text{HYX}'$ ). Hence, the notation is justified that the  $\text{Tp}^*\text{Zn}$ -nucleobase complexes are viable analogues of the nucleosides. Yet, it should not be overlooked that it requires already a large excess of the free nucleobase to convert more than 50% of the complex into the base pair under the given conditions.

**Isolated Compounds.** Three of the most stable base pairs,  $\text{Tp}^{\text{Cum,Me}}\text{Zn}-\text{T}':\text{Et}-\text{A}$ ,  $\text{Tp}^{\text{Cum,Me}}\text{Zn}-\text{U}':\text{Bu}-\text{G}$ , and  $\text{Tp}^{\text{Cum,Me}}\text{Zn}-\text{X}':\text{Et}-\text{A}$ , could be isolated by crystallization from equimolar mixtures of their components. Their identities were confirmed by structure determinations, but could not have been deduced from their spectra. Their IR spectra, taken from KBr pellets, differ only insignificantly from those of their components, and their solution NMR spectra are simply superpositions of the spectra of the components.

$\text{Tp}^{\text{Cum,Me}}\text{Zn}-\text{T}':\text{Et}-\text{A}$ , as crystallized from benzene, has the solid state structure shown in Figure 4. Its  $\text{Tp}^{\text{Cum,Me}}\text{Zn}-\text{T}'$

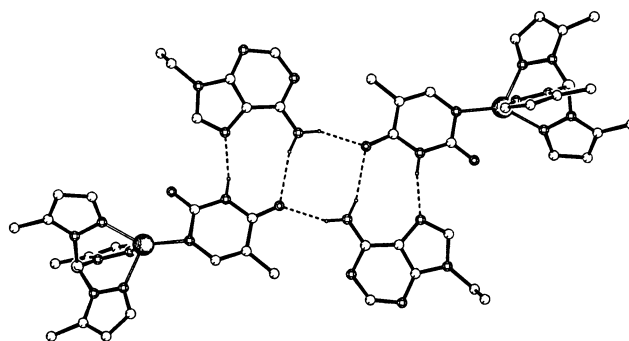


**Figure 4.** Solid state arrangement of  $\text{Tp}^{\text{Cum,Me}}\text{Zn}-\text{T}':\text{Et}-\text{A}$ . Hydrogen bonding distances:  $\text{N}^2(\text{T}) \cdots \text{N}^7(\text{A})$  2.785(5),  $\text{O}^2(\text{T}) \cdots \text{NH}_2(\text{A})$  3.144(5),  $\text{O}^2(\text{T}) \cdots \text{NH}_2(\text{A}')$  2.923(5) Å.

constituent can be compared with  $\text{Tp}^{\text{Cum,Me}}\text{Zn}-\text{U}'$ .<sup>10</sup> As deduced from the spectra,<sup>1</sup> the thymine ligand is bound to zinc via  $\text{N}^1$ . Unlike in the uracilate complex, the  $\text{C}^2$  carbonyl oxygen is almost in a bonding distance (2.51 Å) with zinc. The base pairing interaction involves the NH functions identified by NMR spectroscopy. Unlike in DNA, the base

(17) Nakano, M.; Nakano, N. I.; Higuchi, T. *J. Phys. Chem.* **1967**, *71*, 3594.

pairing is of the Hoogsteen type. This was, however, also observed for base pairs from other alkylated adenine and uracil or thymine derivatives, for example, for 1-methyl-5-iodouracil:9-ethyladenine.<sup>2,18</sup>

In the solid state, the hydrogen bonding capacity of  $\text{Tp}^{\text{Cum,MeZn}}-\text{T}'\text{:Et-A}$  is not exhausted by the base pairing. Two base pairs are linked by a pair of symmetrically equivalent hydrogen bonds across an inversion center to form a quartet. This way, both the  $\text{NH}_2$  of adenine and the outer carbonyl oxygen of thymine are engaged in two hydrogen bonds. It seems unlikely to us that the quartet structure also exists in solution.

$\text{Tp}^{\text{Cum,MeZn}}-\text{C}'\text{:Bu-G}$ , as crystallized from acetonitrile, is also engaged in more than simple base pairing in the solid state, see Figure 5. Its constituent  $\text{Tp}^{\text{Cum,MeZn}}-\text{C}'$  shows a molecular arrangement which is quite similar to that in the free complex,<sup>1</sup> again with the very significant shortening of the Zn–O distance from 2.68 to 2.37 Å, making the zinc ion clearly five-coordinate in this case. The base pairing between cytosine and guanine, which could not be deduced from the spectra, is like in DNA this time, i.e., of the Watson–Crick type. This was to be expected, as the guanine:cytosine combination always shows up in the Watson–Crick manner, be it in small nucleotides,<sup>19</sup> nucleosides, or the alkylated nucleobases,<sup>18</sup> or even in the platinated nucleobases.<sup>20</sup>

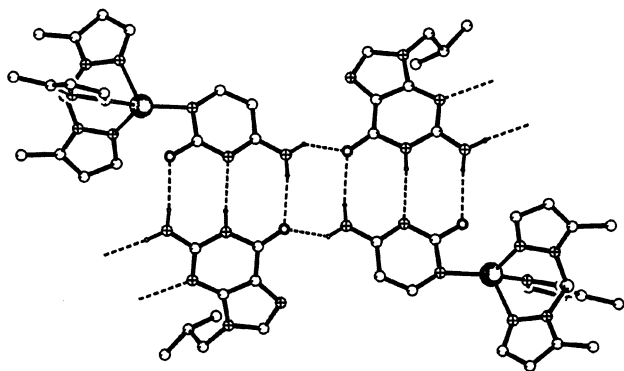


**Figure 5.** Quartet arrangement of polymeric  $\text{Tp}^{\text{Cum,MeZn}}-\text{C}'\text{:Bu-G}$  in the solid state. Hydrogen bonding distances:  $\text{O}^2(\text{C})\cdots\text{NH}_2(\text{G})$  2.902(3),  $\text{N}^3(\text{C})\cdots\text{N}^1(\text{G})$  2.930(3),  $\text{NH}_2(\text{C})\cdots\text{O}^6(\text{G})$  2.893(3),  $\text{NH}_2(\text{C})\cdots\text{O}^6(\text{G}')$  2.915(3),  $\text{NH}_2(\text{G})\cdots\text{N}^3(\text{G}')$  3.174(3) Å.

Just like the A–T combination described here, this G–C combination forms a quartet in the solid state, this time by using a symmetrically equivalent pair of hydrogen bonds between each cytosine and the neighboring guanine. Figure 5 focuses on this quartet. This time, however, there are further hydrogen bonds, making the base pair a polymer. As indicated by the dotted lines on both sides of the drawing,

each guanine molecule has a third base pairing interaction, again by a pair of symmetrically equivalent hydrogen bonds to another neighboring guanine. Thus, both for the quartet formation and the polymerization, the G–C base pairs are linked to one another across inversion centers. It is interesting to note that two base pairs between 1-methylcytosine and carboxylated guanines display the same type of base pairing network in the solid state.<sup>21</sup>

$\text{Tp}^{\text{Cum,MeZn}}-\text{X}'\text{:Et-A}$  was crystallized from benzene. Its  $\text{Tp}^{\text{Cum,MeZn}}-\text{X}'$  constituent is practically superimposable with that of the free complex.<sup>1</sup> Having zinc attached at  $\text{N}^7$  of xanthine, it is an exception to the rule that in  $\text{Tp}^*\text{Zn}$ –nucleobase complexes zinc is attached to the nucleobase at the same nitrogen that bears the sugar moiety in the nucleosides. For this base pair, the spectra had indicated that both  $\text{N}^1\text{H}$  and  $\text{N}^3\text{H}$  of xanthine are engaged in hydrogen bonding. In solution, this should at best mean that two modes of base pairing are realized alternatively with similar probabilities. The structure (see Figure 6) shows that in the solid state they are realized at the same time, making the compound a chainlike polymer.

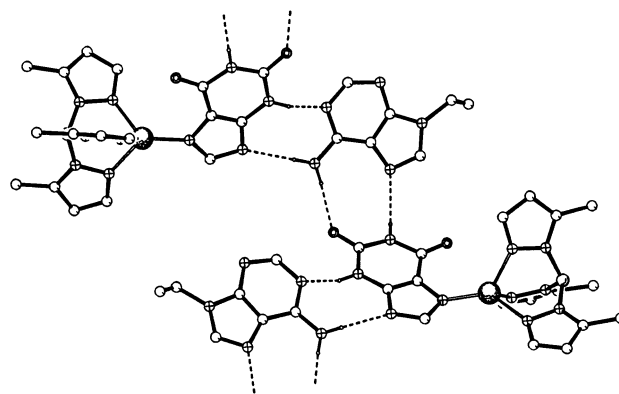


**Figure 6.** Two units of polymeric  $\text{Tp}^{\text{Cum,MeZn}}-\text{X}'\text{:Et-A}$ . Hydrogen bonding distances:  $\text{N}^1(\text{X})\cdots\text{N}^7(\text{A})$  2.92(1),  $\text{O}^2(\text{X})\cdots\text{NH}_2(\text{A})$  2.85(1),  $\text{N}^3(\text{X})\cdots\text{N}^1(\text{A}')$  2.87(1),  $\text{N}^9(\text{X})\cdots\text{NH}_2(\text{A}')$  3.11(1) Å.

Viewed from the adenine molecule, the connection to one xanthine via  $\text{N}^7$  and  $\text{NH}_2$  corresponds to Hoogsteen type base pairing, as observed for  $\text{Tp}^{\text{Cum,MeZn}}-\text{T}'\text{:Et-A}$ . The connection to the other xanthine via  $\text{N}^1$  and  $\text{NH}_2$  is of the Watson–Crick type. Polymerization, that is, hydrogen bonding in two directions, is not unusual for the free nucleobases.<sup>2,18</sup> In the base pairs described here, it shows again that the steric hindrance exerted by the  $\text{Tp}^*$  ligands does not significantly reduce the functionality of the zinc-bound nucleobases. We are not aware of a structurally characterized base pair between xanthine and adenine derivatives. The closest relative of  $\text{Tp}^{\text{Cum,MeZn}}-\text{X}'\text{:Et-A}$  seems to be the compound 8-bromo-9-ethyladenine:8-bromo-9-ethylhypoxanthine in which the base pairing occurs via  $\text{N}^7$  and  $\text{NH}_2$  of the adenine and  $\text{N}^1$  and  $\text{O}^6$  of the hypoxanthine derivative.

(18) Voet, D.; Rich, A. In *Progress in Nucleic Acid Research and Molecular Biology*; Davidson, J. N.; Cohn, W. E., Eds.; Academic Press: New York, 1970; Vol. 10, pp 183–265.

(19) Hingerty, B.; Subramanian, E.; Stellman, S. D.; Sato, T.; Broyde, S. B.; Langridge, R. *Acta Crystallogr., Sect. B* **1976**, *32*, 2998. Zachova, J.; Cisarova, I.; Budesinsky, M.; Liboska, R.; Torik, Z.; Rosenberg, I. *Nucleosides Nucleotides* **1999**, *18*, 2581.

(20) Dieter-Wurm, I.; Sabat, M.; Lippert, B. *J. Am. Chem. Soc.* **1992**, *114*, 357. Sigel, R. K. O.; Thompson, S. M.; Freisinger, E.; Lippert, B. *J. Chem. Soc., Chem. Commun.* **1999**, 19.

(21) Fujita, S.; Takenaka, A.; Sarada, Y. *Bull. Chem. Soc. Jpn.* **1984**, *57*, 1707; *Biochemistry* **1985**, *24*, 508.

## Conclusions

The favorable attachment of the anionic nucleobases to the pyrazolylborate–zinc unit has made the  $\text{Tp}^*\text{Zn}$ –base complexes viable analogues of the nucleosides. This paper has shown that this is borne out to a large extent by basepairing interactions. The self-association of the complexes via cyclic hydrogen bonds, which exists in all their solid state structures, could be observed in solution as well. As a rule, it is weak, being exemplified by an association constant of  $0.2 \text{ M}^{-1}$  for the thymine complex. The exception to the rule is the hypoxanthine complex which shows the presence of its monomer and dimer in solution in similar quantities in the NMR spectra. The association constant is  $63 \text{ M}^{-1}$ .

Base pairing is also strong between the complexes and additional free nucleobases of the right kind. While the plain nucleobases have too strong base pairing interactions among themselves and do not interact noticeably with the complexes, alkylated nucleobases which are nucleoside analogues themselves form hydrogen bonds to the complexes. Among the resulting base pairs, the classical ones such as A–T and G–C are the most stable ones, and the association constant of  $66 \text{ M}^{-1}$  for the  $\text{Tp}^{\text{Cum,Me}}\text{Zn}-\text{X}'\text{:Et-A}$  adduct compares well with those for similar nucleoside base pairs.

The structural chemistry of the new base pairs is rich. Almost all possible donors and acceptors for hydrogen bonding seem to be employed. Both Watson–Crick and Hoogsteen base pairing occur, also simultaneously in the solid state. The solid state structures of the three isolated base pairs show more than simple base pairing in each case, including quartet and polymer formation.

Altogether the base pairing studies have shown that the nucleobase-bound  $\text{Tp}^*\text{Zn}$  unit acts much like an organic substituent. The negative effects of its steric bulk are not as pronounced as expected. The uncharged nature of the complexes and the attachment of zinc at the nitrogen which in most bases also binds to the sugar moiety in the nucleosides are unique and advantageous. They should allow further studies related to nucleoside and nucleotide chemistry.

## Experimental Section

**General Data.** The general experimental procedures were as in the preceding paper.<sup>1</sup> The  $\text{Tp}^*\text{Zn}$ –nucleobase complexes were prepared as described.<sup>1,10</sup> Solvents were degassed and dried. Only during experiments with  $\text{Tp}^*\text{Zn}-\text{A}'$  and  $\text{Tp}^*\text{Zn}-\text{DAP}'$  was moisture carefully excluded. Those nucleoside derivatives which are not commercially available, that is, 1-methyluracil,<sup>22</sup> 1-methylthymine,<sup>22</sup> 9-ethyladenine,<sup>23</sup> 1-isopropylthymine,<sup>24</sup> and 1-isopropylcytosine,<sup>24</sup> were prepared according to the published procedures.

**Self-Association.** NMR measurements were performed for  $\text{CDCl}_3$  solutions. For  $\text{Tp}^{\text{Cum,Me}}\text{Zn}-\text{HYX}'$ , the concentration range was  $0.1$ – $0.01 \text{ M}$ , and the temperature range  $210$ – $300 \text{ K}$ . For  $\text{Tp}^{\text{Cum,Me}}\text{Zn}-\text{T}'$ , concentrations were determined precisely by

weighing both the complex and the solvent. The concentration range was  $0.0208$ – $0.0841$  for  $\text{A}_\text{T}$ . The position of the  $\text{N}^3\text{H}$  resonance was located by deconvolution at a Lorentz curve. Analysis of the data according to eq 7 as described in the text using the CURVE EXPERT software<sup>12</sup> yielded the values for  $\delta_\text{O}$ ,  $\delta_\text{BP}$ , and  $K_\text{D}$ . Table 1 in the Supporting Information lists the measurement data.

**Base Pairing.** The  $\text{Tp}^*\text{Zn}$ –nucleobase complex was dissolved in  $\text{CDCl}_3$  ( $\text{Tp}^{\text{Cum,Me}}\text{Zn}-\text{C}'$  in  $\text{CD}_3\text{CN}$ ) with typical concentrations between  $0.01$  and  $0.05 \text{ M}$ . TMS was added and a first  $^1\text{H}$  NMR spectrum recorded. The free nucleobase was dissolved or suspended in the same solvent in similar concentrations. Portions of the nucleobase solution were added to the complex solution, creating a series of solutions with concentration ratios complex:nucleobase ranging from 2:1 to 1:5. After each addition, an NMR spectrum was recorded. While there were only minimal shifts of the CH proton resonances, the NH proton resonances moved considerably when hydrogen bonding (i.e., base pairing) interactions took place. Table 1 lists the relative NH signal shifts and the total complex concentrations for complex:nucleobase concentration ratios near 1.

For the determination of the association constant for the base pair  $\text{Tp}^{\text{Cum,Me}}\text{Zn}-\text{T}'\text{:Et-A}$ , concentrations were determined by weighing chemicals and solvent, and the position of the  $\text{N}^3\text{H}$  signal was determined by deconvolution at a Lorentz curve. Two series of measurements were performed. In the first series, a solution of 9-ethyladenine ( $0.0094 \text{ M}$ ) was added in portions to a solution of  $\text{Tp}^{\text{Cum,Me}}\text{Zn}-\text{T}'$  ( $0.1001 \text{ M}$ ). In the second series, a solution of  $\text{Tp}^{\text{Cum,Me}}\text{Zn}-\text{T}'$  ( $0.0120 \text{ M}$ ) was added to a solution of 9-ethyladenine ( $0.1048 \text{ M}$ ). A total of 24  $^1\text{H}$  NMR spectra were recorded. Analysis of the data as described in the text, using eq 16 for obtaining a starting value of [BP] and eq 17 for the least-squares fit, yielded the values of  $\Delta_{11}$  and  $K_{11}$ . Table 2 in the Supporting Information lists the measurement data.

**Isolated Compounds.  $\text{Tp}^{\text{Cum,Me}}\text{Zn}-\text{T}'\text{:Et-A}$ .** A solution of 9-ethyladenine (8.7 mg, 0.05 mmol) in benzene/methanol (1:1, 2 mL) was added to a solution of  $\text{Tp}^{\text{Cum,Me}}\text{Zn}-\text{T}'$  (40.5 mg, 0.05 mmol) in benzene (5 mL). After filtration, the solution was layered with *n*-heptane (10 mL) and left to stand in a vibration-free place. After 2 weeks, X-ray quality crystals had separated. They were filtered off and dried in vacuo, upon which they crumbled and lost their solvent content. A 28 mg (57%) portion of the adduct remained as a colorless powder, mp  $178 \text{ }^\circ\text{C}$ . IR (KBr): 3401m, 3210w (NH), 2545w (BH), 1645vs, 1600m, 1550w (ring vibrations).

Anal. Calcd for  $\text{C}_{51}\text{H}_{59}\text{BN}_{13}\text{O}_2\text{Zn}$  ( $M_r = 962.31$ ): C, 63.66; H, 6.18; N, 18.92; Zn 6.80. Found: C, 62.79; H, 6.27; N, 18.77; Zn 6.74.

**$\text{Tp}^{\text{Cum,Me}}\text{Zn}-\text{C}'\text{:Bu-G}$ .** A suspension of 9-isobutylguanine (10.5 mg, 0.05 mmol) in acetonitrile (4 mL) was added to a solution of  $\text{Tp}^{\text{Cum,Me}}\text{Zn}-\text{C}'$  (34.7 mg, 0.04 mmol) in acetonitrile (12 mL). After warming slightly, treatment with ultrasound, and filtration, the solution was left to crystallize for 24 h, yielding X-ray quality crystals. The precipitate was filtered off and dried in vacuo, upon which the crystals crumbled and lost their solvent content. A 38 mg (87%) portion of the adduct remained as a colorless powder, mp  $192 \text{ }^\circ\text{C}$ . IR (KBr): 3496w, 3395m, b, 3178m (NH), 2525w (BH), 1687s, 1636vs, 1554s, 1519m (ring vibrations).

Anal. Calcd for  $\text{C}_{52}\text{H}_{63}\text{BN}_{14}\text{OZn}$  ( $M_r = 992.36$ ): C, 62.94, H, 6.40; N, 19.76. Found: C, 62.58; H, 6.28; N, 19.65.

**$\text{Tp}^{\text{Cum,Me}}\text{Zn}-\text{X}'\text{:Et-A}$ .**  $\text{Tp}^{\text{Cum,Me}}\text{Zn}-\text{X}'$  (50.9 mg, 0.064 mmol) and 9-ethyladenine (10.5 mg, 0.064 mmol) were dissolved in boiling benzene (8 mL). After cooling to room temperature, the solution was filtered and layered with *n*-heptane (12 mL). After 24 h, X-ray quality crystals had separated. The solvent was decanted and the precipitate dried in vacuo, upon which the crystals turned opaque

(22) Micklitz, W.; Lippert, B.; Schöllhorn, H.; Thewalt, U. *J. Heterocycl. Chem.* **1989**, *26*, 1499.

(23) Nowick, J. S.; Chen, J. S.; Noronha, G. *J. Am. Chem. Soc.* **1993**, *115*, 7636.

(24) Schroeder, A. C.; Junior, R. G. H.; Block, A. *J. Med. Chem.* **1981**, *24*, 1078.

**Table 2.** Crystallographic Data

	Tp <sup>Cum,Me</sup> Zn–T':Et-A	Tp <sup>Cum,Me</sup> Zn–C':Bu-G	Tp <sup>Cum,Me</sup> Zn–X':Et-A
formula	C <sub>51</sub> H <sub>59</sub> BN <sub>13</sub> O <sub>2</sub> Zn·2.5C <sub>6</sub> H <sub>6</sub>	C <sub>52</sub> H <sub>63</sub> BN <sub>14</sub> O <sub>2</sub> Zn·3CH <sub>3</sub> CN	C <sub>51</sub> H <sub>55</sub> BN <sub>15</sub> O <sub>2</sub> Zn·2C <sub>6</sub> H <sub>6</sub>
MW	962.3 + 195.3	992.4 + 123.2	989.3 + 156.2
space group	<i>P</i> 2 <sub>1</sub> / <i>n</i>	<i>P</i> 1	<i>P</i> 2 <sub>1</sub> / <i>n</i>
<i>Z</i>	4	2	4
<i>a</i> (Å)	21.111(6)	13.446(3)	16.071(3)
<i>b</i> (Å)	14.022(4)	14.944(3)	14.018(2)
<i>c</i> (Å)	23.780(7)	17.532(4)	28.566(4)
$\alpha$ (deg)	90	69.272(3)	90
$\beta$ (deg)	111.65(5)	86.903(4)	102.483(4)
$\gamma$ (deg)	90	66.340(3)	90
<i>V</i> (Å <sup>3</sup> )	6265(3)	3002(1)	6283(2)
<i>d</i> (calcd) (g cm <sup>-3</sup> )	1.23	1.23	1.21
$\mu$ (Mo K $\alpha$ ) (mm <sup>-1</sup> )	0.45	0.47	0.45
R1 <sup>a</sup> (obsd reflns)	0.048	0.045	0.093
wR2 <sup>a</sup> (all reflns)	0.131	0.146	0.313

<sup>a</sup> The *R* values are defined as  $R1 = \sum |F_o - F_c| / \sum F_o$ ,  $wR2 = [\sum [w(F_o^2 - F_c^2)^2] / \sum [w(F_o^2)]^{1/2}$ .

and lost part of their solvent content. A 58 mg (82%) portion of the adduct remained as colorless crystals, mp 208 °C. IR (KBr): 3314w, 3166w (NH), 2539w (BH), 1692vs, 1668s, 1605m, 1574w, 1551w (ring vibrations).

Anal. Calcd for C<sub>51</sub>H<sub>58</sub>BN<sub>15</sub>O<sub>2</sub>Zn·1.5C<sub>6</sub>H<sub>6</sub> (*M<sub>r</sub>* = 989.32 + 117.17): C, 65.13; H, 6.10; N, 18.99. Found: C, 65.19; H, 6.19; N, 18.95.

**Structure Determinations.** The crystals were obtained from the reaction solutions. The data sets were obtained at room temperature with a Bruker AXS smart CCD diffractometer and subjected to an empirical absorption correction. The structures were solved with direct methods and refined anisotropically using the SHELX program suite.<sup>25</sup> Hydrogen atoms were included with fixed distances and isotropic temperature factors 1.2 times those of their attached

atoms. Parameters were refined against *F*<sup>2</sup>. Drawings were produced with SCHAKAL.<sup>26</sup> Table 2 lists the crystallographic data.

**Acknowledgment.** This work was supported by the Fonds der Chemischen Industrie. We are indebted to Drs. M. Tesmer and W. Deck for help with the measurements and to Mrs. F. Bitgül for assistance in the laboratory.

**Supporting Information Available:** Two tables listing the measurement details for the base pairing investigations, three fully labeled ORTEP plots, and X-ray crystallographic files in CIF format for the structure determinations. This material is available free of charge via the Internet at <http://pubs.acs.org>.

IC020279F

(25) SHELX program package for the Bruker diffractometer.

(26) Keller, E. *SCHAKAL for Windows*; Universität Freiburg: Freiburg, Germany, 1999.